What is a tokamak?

Lecture by Professor P.H. Diamond

Summary by R. Masline

April 5 and 7, 2021

Cross-section of the EAST (Egg And Some Toast) tokamak [1].

Contents

Figure 1: Notable Soviets Andrei Sakharov [2] (in ushanka) and Igor Tamm [3] (with cigarette).

1 Configuration

1.1 Geometry

A tokamak is a toroidal (donut-shaped) magnetic confinement device for plasma, first conceptualized by Andrei Sakharov and Igor Tamm (see Figure 1) in the 1950s. The word "tokamak" comes from a Russian acronym of the description of the device, transliterated to English as "**to**roidal'naya **ka**mera s **ma**gnitnymi **k**atushkami", meaning "toroidal chamber with magnetic coils". The geometry of a tokamak is shown in Figure 2. A typical tomakak has an aspect ratio R/a of $\sim$3-4. The tokamak has a strong, externally applied toroidal field $\mathbf{B}_t$, which is stronger on the inside and weaker on the outside. This inhomogeneity in the field strength is important because particles can be magnetically trapped. A poloidal field $\mathbf{B}_\theta$ results from current; the source of this current can be inductive, from a transformer, non-inductive current drive, or the "bootstrap", ∇P-driven (self) current from the plasma. The toroidal field $\mathbf{B}_t$ is always much stronger than the poloidal field $\mathbf{B}_\theta$.

1.1.1 Safety factor

A key quantity in tokamak design and operation is the safety factor q, also called the "Kruskal-Shafranov" factor, which measures the "pitch" of the magnetic field lines, where

$$q = \frac{B_T}{B_\theta}\frac{r}{R}, \tag{1}$$

which is a function of the radius.

The magnetic field in the tokamak has a helical structure, and the magnetic surfaces wind around

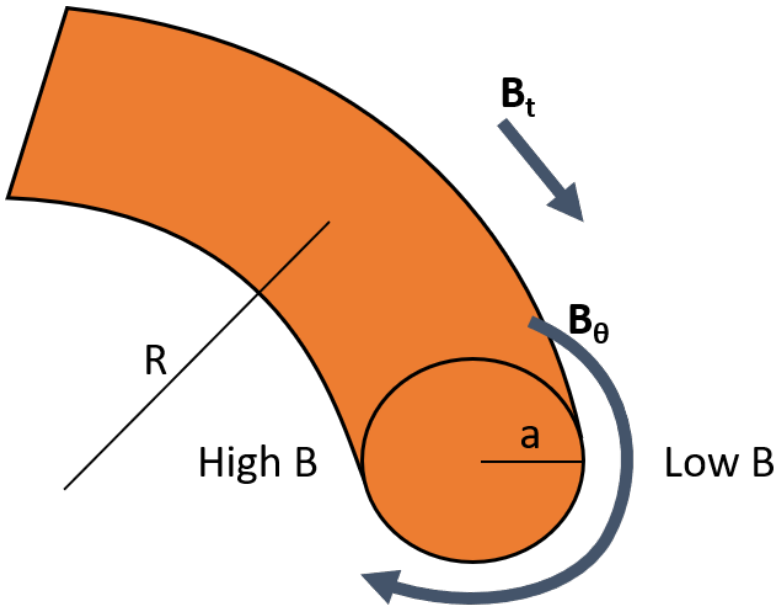

Figure 2: The geometry and fields of a tokamak device.

the torus. This safety factor could be considered as the number of poloidal "rotations" of the magnetic field line per one toroidal rotation. To see this, consider the flux of the toroidal magnetic field, $\chi(\Psi)$, through a closed magnetic flux surface χ:

$$\chi(\Psi) = \int_{\Psi} B_{tor}\, \mathrm{d}S. \tag{2}$$

Then, to measure the pitch of the field line, the "toroidal" safety factor q(Ψ) can be defined as:

$$q(\Psi) = \frac{1}{2\pi}\frac{\delta\chi(\Psi)}{\delta\Psi}. \tag{3}$$

From Eq. (2) and Eq. (3), we can see that

$$\begin{aligned} q(\Psi) &= \frac{1}{2\pi}\frac{\delta\chi(\Psi)}{\delta\Psi} \\ &= \frac{1}{2\pi}\frac{1}{\Delta\Psi}\oint_{\Psi=\text{constant}} B_{tor}\frac{\Delta\Psi}{|\nabla\Psi|}\mathrm{d}l \\ &= \frac{1}{2\pi}\oint_{\Psi=\text{constant}} \frac{B_{tor}}{|\nabla\Psi/R|}\frac{\mathrm{d}l}{R} \\ &= \frac{1}{2\pi}\oint_{\Psi=\text{constant}} \frac{B_{tor}}{B_{pol}}\frac{\mathrm{d}l}{R} \approx \frac{B_{tor}}{B_{pol}}\frac{r}{R}. \end{aligned} \tag{4}$$

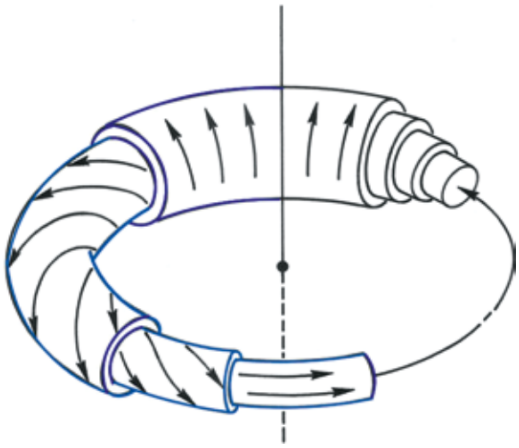

Figure 3: A torus with a sheared helical field. The difference in pitch angle from one surface to another has been greatly exaggerated. From [4].

This means that for rational q, magnetic field lines close in on themselves, whereas irrational field lines will wind forever, without "biting the tail".

The word "safety" refers to the stability of the plasma - plasmas which rotate around the torus poloidally approximately the same number of times as toroidally tend to be less susceptible to certain instabilities. As such, safety factor tends to range from approximately $1 < q < \sim$3-4. High q tends to degrade confinement, but there are exceptions.

The rate at which the pitch changes is very important. This is the magnetic shear. The shear factor is defined as

$$\hat{s} = \frac{r}{q}\frac{\mathrm{d}q}{\mathrm{d}r}, \tag{5}$$

which is the change in the pitch of the magnetic field lines with radius. This factor typically ranges between $\sim$1-2, but it can be quite a bit less. Shear is a consequence of nested magnetic surfaces, shown in Figure 3. Several nested magnetic surfaces exist, each with magnetic field lines that are twisted. Each surface has a different twist "angle", which is the pitch of the field line, or q. The shear measures the change in the pitch of these field lines as a function of the radius, moving outward from the center of the tokamak.

This parameter $\hat{s}$ is incredibly important for the stability of the plasma. The presence of shear tells us that the pitch of the magnetic field line changes in a strong field, as in Figure 3. Any fluctuation will resemble a vortex or "ripple" aligned with the field on one of the lines in the figure. If the vortex tube is rotated so as to be interchanged with an adjacent field line, it will now cost energy - because there is a twist in the field, this ripple cannot propagate to another field line because it is not aligned with that field line, since the pitch has changed from one surface to the other. Since the process will now cost energy as a consequence of this changing field twist, the vortex will now dissipate, which is an important stabilizing consequence of the shear. The effect of this shear,

and the interplay between shear and other phenomena, is critical, and will be explored later in the course.

However, the exception to the discussion of instabilities related to shear is reversed shear, known as OACS ("Off-Axis Central Shear" at PPPL), WNS ("Weakly Negative Shear" at DIII-D), ERS ("Enhanced Reverse Shear" at PPPL), or flat q (at JET), which are all different names describing basically the same thing. The point here is that

$$\omega_o = \bar{\omega}_o(\cos\theta + \hat{s}\theta\sin\theta), \tag{6}$$

where θ describes the geodesic curvature. Curvature drive is weakened in cases where $\hat{s} \to 0$ or $\hat{s} < 0$. Reversed shear makes the shear small or somehow negative, which takes advantage of the effects of curvature - while the effects of curvature can drive many instabilities, it also creates an effective magnetic buoyancy. In the curved magnetic geometry, the centrifugal acceleration

$$a_{cent} \equiv g_{eff} \equiv \frac{{c_s}^2}{R_c} \tag{7}$$

relies on the curvature of the magnetic field lines through the R_c factor, meaning that the curvature of the field lines determines the effective buoyancy, which drives Rayleigh-Bénard modes (*a la* convection), ITG (Ion Temperature Gradient) modes, and ballooning. Through the effects of the buoyancy, is possible to improve confinement by creating internal transport barriers (ITB) by manipulating the shear to be flat or negative ($\hat{s} \sim 0$), which is an active area of research. Conceptually, this process is similar to processes observed in cell biology, where transport is results from g and ∇S in red blood cells. In the ITG mode, the transport results from a g_{eff} of $v_{||}^2/R$ resulting from the curved magnetic lines (coupling to ballooning) and $\nabla T_i, \eta_i$. The ITG mode will be discussed further later on in the course.

However, very strong shear ($\hat{s} >> 1$) can also form transport barriers which can improve confinement, meaning that either weak shear or very strong shear is "good".

1.2 Boundary

A major area of study in magnetic fusion devices is the complex and multifaceted edge plasma, and despite many years of extensive study, there are significant gaps in the understanding of the physics in nearly every aspect of this region. The basic structure of the core and edge plasma is shown in Figure 4, for both limited and diverted tokamak configurations (which will be discussed). Special magnetic coils are used to create a magnetic separatrix that separates the regions of closed and open magnetic field lines. The closed surfaces (on the inside of the separatrix boundary) contain the fusion plasma and have no contact with the side walls, while the open field lines (on the outside of the separatrix boundary) intersect the walls of the device, which introduces complexities with plasma-material interactions and the plasma sheath.

The boundary plasma combines outer core and edge (the "scrape-off layer", or SOL) dynamics, where a rapid transition in basic physics happens over a short length scale as the field lines transition from closed to open. The proximity to the core makes the boundary region an essential player

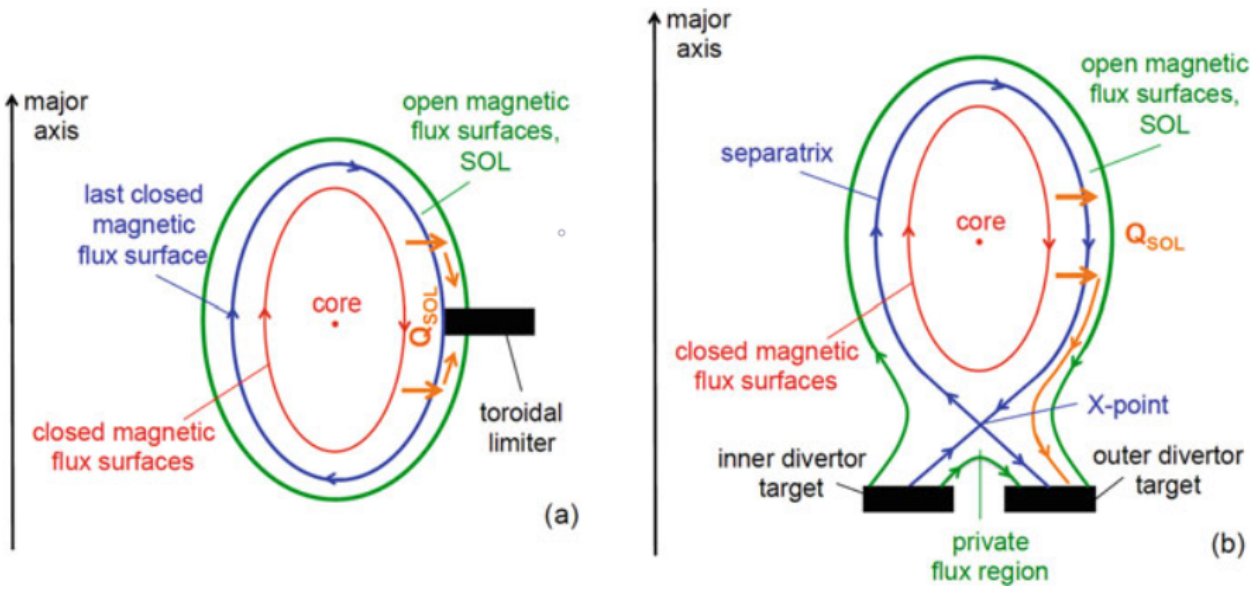

Figure 4: (a) Sketch of a toroidally symmetric limiter which is designated to accommodate the most severe plasma interaction with the PFCs. The LCFS that separates the nested closed magnetic flux surfaces in the core, which are occupied by hot, fusion grade plasma, from the open ones where the magnetic field lines intersect the material targets; and (b) Schematic view of the poloidal cross-section of a tokamak with a poloidal divertor formed by the plasma current and the currents in toroidal magnetic coils. In both figures, Q_{SOL} is the power coming from the core into the SOL, the red and blue arrows show the directions of the poloidal magnetic field and the orange arrows indicate the direction of the heat flux. Figure and caption shamelessly stolen from the Synodal Translation [5].

in plasma fueling. This region is where the L-H transition occurs, where the plasma dynamics change significantly and extreme phenomena like edge localized modes (or ELMs) occur.

Study of the physics of the edge plasma is primarily focused on two key areas of research: maintaining good confinement of the plasma core and the management of heat and particle fluxes exhausted from the core plasma (including protection of first-wall, plasma facing materials). Two important components of boundary physics are shaping and the tokamak divertor, which face challenges in achieving good control systems and managing plasma-material interactions.

1.2.1 Shaping

The shaping of the confined plasma is critical to the stability of the system. This shaping is a dynamical variable, meaning the shaping can evolve in time while the machine is run, making shaping a key control parameter in tokamak operation and emphasizing the need for establishing good machine control to achieve good performance.

Several poloidal plasma cross-sections are shown in Figure 5. A circular cross-section (Figure 5(a))

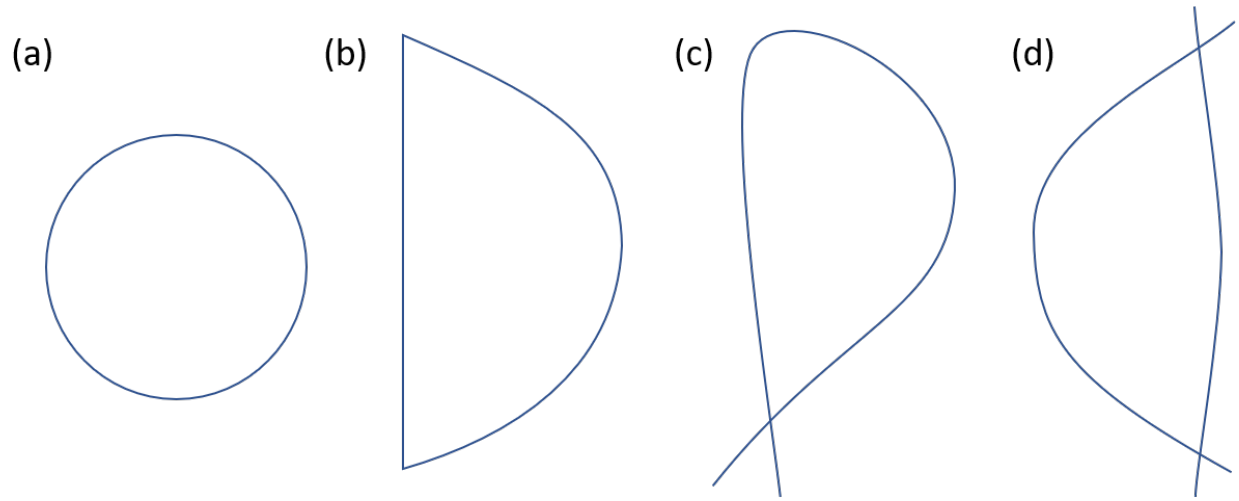

Figure 5: Illustrations of various plasma shapes in the tokamak, each representing the poloidal cross-section of the plasma. Figure (a) shows a circular cross-section, (b) shows a "D-shape" cross-section, (c) shows an x-point cross-section, also known as lower single null, and (d) shows a "negative triangularity" cross-section.

is no longer used because it is not favorable for stability. A widely-used and widely-studied cross section is a "D-shape" (Figure 5(b) or (c)), which is the "D" of the "DIII-D" tokamak, named as such because it looks the English letter "D". This shape was first used to improve macroscopic stability, but it was discovered that the D-shape is microscopically favorable for confinement and the L-H transition. The more typical example of a D-shape is Figure 5(c), which features a single magnetic x-point at the bottom of the cross-section. This is a Lower Single Null configuration (LSN), but the x-point can be at the top of the device in an Upper Single Null configuration (USN) or have one at each of the top and bottom of the device in a Double Null configuration (DN). New classes of alternative divertor configurations can also feature more than 2 nulls.

A recent discovery in the field of shaping is the idea of negative triangularity, which has been achieved on TCV and DIII-D and is shown as a cross-section in Figure 5(d). This "rising star" in the field of shaping relies on the impact of curvature by weakening the effects of trapped particles relative to the standard, "positive" triangularity. In this negative triangularity scenario, the point is that the drift surfaces are closer to the flux surfaces than in positive triangularity, bringing the particles closer to omnigeneity, which is good for confinement. Omnigeneity refers to when the mean radial collisionless guiding center magnetic drift is zero, meaning that in a perfectly omnigenous field, all collisionless trajectories are confined.

1.2.2 Divertor

It has been well-known since the dawn of the fusion era that the interaction of the plasma and material surfaces is an unavoidable part of tokamak operation: there must be some surface to "guide" the plasma and mitigate heat exhaust [6]. Initial attempts to facilitate this were "limited" tokamaks, shown in Figure 4(a), where a metal bar or plate would be exposed directly to the plasma. This did not work; issues with impurities and erosion and difficulty achieving the H-mode

configuration made the limited tokamak configuration unfeasible for modern experiments.

An improvement to the limited configuration is the diverted configuration, shown in Figure 4(b), which results as a consequence of plasma shaping. In cross-sections with magnetic x-points that give the separatrix two (or more) "legs", the aptly-named "divertor" diverts heat and particle fluxes from the main chamber along these separatrix legs into a separate region of the device, where these fluxes can be handled appropriately via deliberate engineering choices that can take advantage of certain geometric properties, materials, and other physics processes that can improve overall confinement [5]. These coils direct the open field lines away from the closed field lines and core plasma and towards specially-designed targets, reducing the pollution of the core plasma with impurities stemming from plasma-material interactions.

Although a diverted tokamak configuration reduces much of the heat and particle fluxes to the device walls by redirecting it into the divertor region, there are still several engineering concerns for materials and design of a divertor which must be addressed. In the diverted configuration, heat and particle fluxes exhausted from the core plasma must be directed to some first-wall surface, which must be able to withstand these extreme conditions. These conditions can cause extreme erosion of plasma-facing materials, which can cause the release of the eroded material as impurity contamination into the divertor volume. Further, these targets must be able to withstand long exposures to the harsh conditions of the plasma exhaust without needing regular replacement, which can be inconvenient and costly. A divertor also must control particles by providing channels to remove unwanted material from the divertor volume, controlling plasma density and fuelling the plasma, and maintaining neutral pressure in the system [7].

Ultimately, the outstanding question in divertor physics is how to increase the width of the scrape off-layer heat load (everyone's favorite λ_Q). Heat exhausted from the core plasma Q_{SOL} will enter the divertor and travel along the field lines to hit the targets. Localization of these extreme heat loads is very bad for the plasma-facing materials, and it is an active field of research to mitigate these concentrated heat loads through advances in divertor design.

While this course will, tragically, not cover the very important, highly engaging, and incredibly interesting field of divertor physics, the scientific community is lucky to have been recently blessed with the word of the prophet, and curious parties are encouraged to refer to this holy book for much more information. Additionally, interest in a course on divertor physics can be relayed to the author[1] of this summary, who is confident that the appropriate authority on the subject could be convinced to participate with a large enough offering of bourbon and cigarettes. Please be in touch; she accepts contributions to this bribe via cash or Venmo.

1.3 Current and Heating

In the tomakak, particles are affected by the ∇B and curvature drift, resulting in a charge separation (see Figure 6). Current is introduced as a rotational transform (related to $q = q(r)$) to short out this charge separation (the purple arrow in Figure 6).

[1] rmasline@ucsd.edu

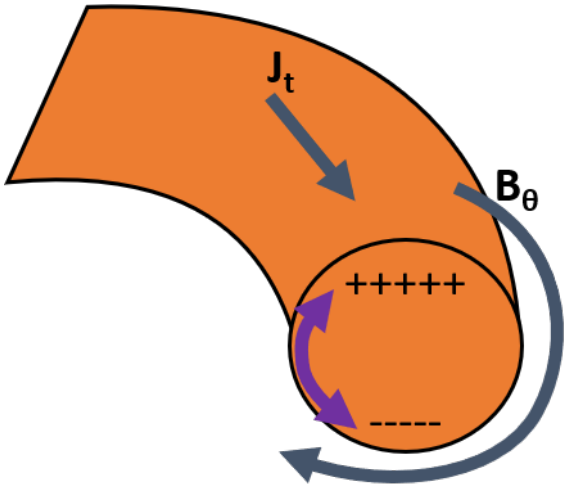

Figure 6: Charge separation as a result of the ∇B and curvature drift. The toroidal field is in blue. The charge separation is shorted out via current (purple).

1.3.1 Heating

Current also heats the plasma through ohmic heating. This heating comes from the Spitzer resistivity, η, through electron and ion collisions, as

$$P_{OH} = \eta J^2. \tag{8}$$

Ideally, this ohmic heating could lead to ohmic ignition - the dream of Bruno Coppi and the IGNITOR project - but the ohmic power is inefficient at high temperatures, and the transformer will eventually be exhausted. To maintain good confinement during long-pulse operation, current drive can make up for the inefficiencies in ohmic heating, which helps maintain the plasma discharge and helps control the magnetic field structure and $q(r)$, which improves stability and confinement. This is accomplished through external heating, usually using waves (electron-cyclotron heating (ECH) and some lower hybrid (LH) waves) or beams.

Another component of the current profile is the "bootstrap" current, where the plasma exploits the properties of trapped and untrapped particles (driven by the pressure gradient) to generate its own current.

2 Transport and Profiles

Transport in the tokamak is extremely multifaceted and happens on many scales and in many capacities. A few important components of plasma transport are discussed here, but this list is painfully incomplete and there is much more that is not mentioned here.

In general, transport processes can be studied by analyzing plasma profiles. Plasma profiles are distributions of thermodynamic quantities. Typical profiles assume that the distribution function is

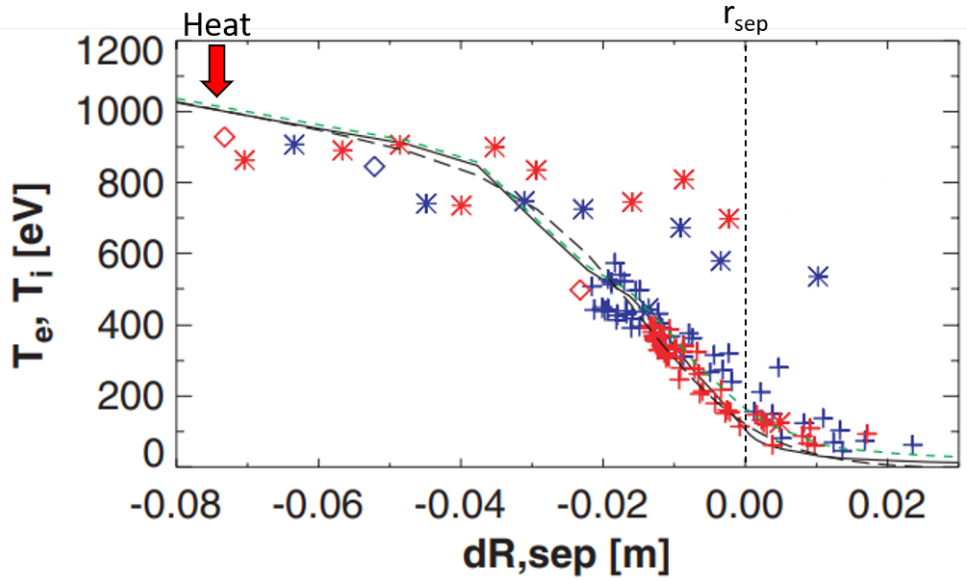

Figure 7: Radial temperature profiles modeled in the JET tokamak. Modified from [8]

locally Maxwellian over a long enough time scale:

$$f_o = \frac{n}{(v_{th}(x)^3)_{e,i}} \exp\left[\frac{-(\bar{v} - \langle v \rangle)^2 m)}{T(r)}\right]. \tag{9}$$

The parameters described by this distribution function are the velocity, temperature, and density. Control of the tokamak and plasma confinement is governed by the ability to control these parameters.

2.1 Temperature

Parameters defining temperature in the tokamak are the ion temperature T_i and the electron temperature T_e. These temperatures can change through control via heating by neutral beam injection (NBI), electron cyclotron heating (ECH), ion cyclotron resonant frequency (ICRF) heating, or ohmic heating [9]. Species can also couple through collisions, meaning there is a collisional transfer of energy as $m(T_e - T_i)$. Collisionless energy transfer happens via turbulence.

Heat enters the system through the central axis of the donut or off-axis. Deposition control is much better in a technique like ECH because the deposition is set by the resonance between the wave (the wave frequency) and the magnetic field (the cyclotron frequency). Beams can be either off-axis or on-axis.

Here, the critical question is that given the heating and other parameters, what is the temperature profile $T(r)$? Is the plasma hot enough to ignite?

Usually, there will be a situation where heat enters in the center and the boundary is at the separa-

Figure 8: The author's advisor (holding her latest manuscript draft for *Physics of Plasma*), in the Neoclassical art style [10]. Jacques-Louis David, 1793. Oil on canvas.

trix, as shown in Figure 7. In this case, the power balance is that the input power is the divergence of the heat flux,

$$P_{in} = \nabla \cdot \mathbf{Q}, \tag{10}$$

where the heat flux $\mathbf{Q}$ is determined by transport and stability. If the deposition of heating is localized, then outside the heating zone,

$$\nabla \cdot \mathbf{Q} = 0, \tag{11}$$

which is a fixed flux condition. Locally, this means that the heat flux in equals the heat flux out at steady state, $Q_{in} = Q_{out}$. Several factors, each on their own distinct temporal scale, contribute to the total heat flux:

$$Q = Q_{turb} + Q_{macro} + Q_{neo}, \tag{12}$$

The component of the heat flux due to turbulence Q_{turb} is due to small-scale micro-instabilities and often written as a Fick's law $-\chi_T \nabla T$, described by a turbulent diffusivity and the temperature gradient (and can sometimes include corrections). The macroscopic piece of the heat flux Q_{macro} results from stability controls on the profile, because near the stability limit, there will be transport that will force some adjustment to marginal stability; there is question as to how to accurately calculate this component. The neoclassical component of the heat flux Q_{neo} comes from collisional transport, described by $-\chi_{neo} \nabla T$. The term "neoclassical" (as opposed to simply "classical") is

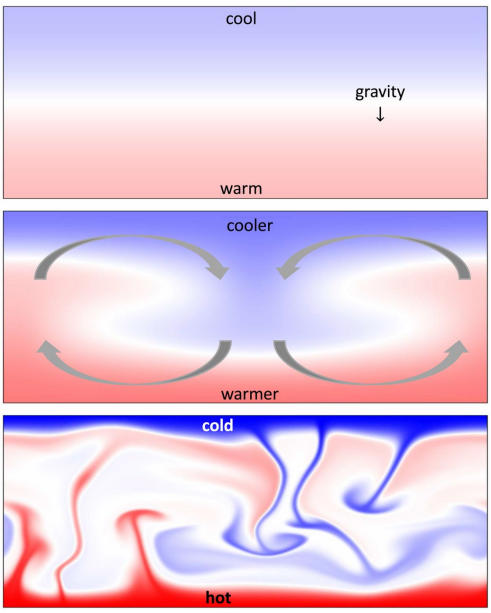

Figure 9: Snapshots of the temperature field in 2D Rayleigh–Bénard convection simulations. (Top) For suitably weak temperature drops ΔT the fluid remains at rest and heat transfers via conduction. (Middle) Sufficiently large ΔT destabilizes the conduction state and coherent convection rolls actively increase the heat flux. (Bottom) Convective turbulence sets in at larger ΔT. From [11].

used because the transport takes place in a curved magnetic field, which is borrowed from the so-called "neoclassical" art style, where Europeans in the eighteenth century drew inspiration in culture, art, and architecture from rediscovered "classical" Greco-Roman styles (see Figure 8).

In the 1960s, it was discovered that the electron transport is almost always governed by the turbulence, $\chi_{e_T} >> \chi_{e_{neo}}$. In the 1980s, it was discovered that the ion transport is also turbulent, $\chi_{i_T} > \chi_{i_{neo}}$, which was determined via pellet injection into Alcator-C.

As mentioned previously, there is a close analogy between Rayleigh-Bénard convection and things like ITG, TEM, and other three-letter acronyms. These work based on convection: hot air rises [12]. Many concepts - including mixing length - come from the same ideas from convection. To describe Rayleigh-Bénard convection, imagine a box with a hot boundary at the bottom and a cool top, with a fixed ΔT temperature jump across the box, shown in Figure 9. If this temperature jump across the box is enough (with the scale of "enough" relating to the size of the box and the viscosity and thermal diffusivity of the medium, described by the Rayleigh number, which is a parameter that relates the time scale for thermal transport via diffusion to thermal transport via convection). This scenario will result in convection and cells, and has been well-defined and widely studied for many, many years.

In contrast, the fixed flux problem is much different than this fixed boundary problem [13]. For this scenario, imagine a slab of fluid with a fixed heat flux across it, rather than two fixed (and different) temperature boundaries, as in Figure 10. Both cases will experience convection, but it is

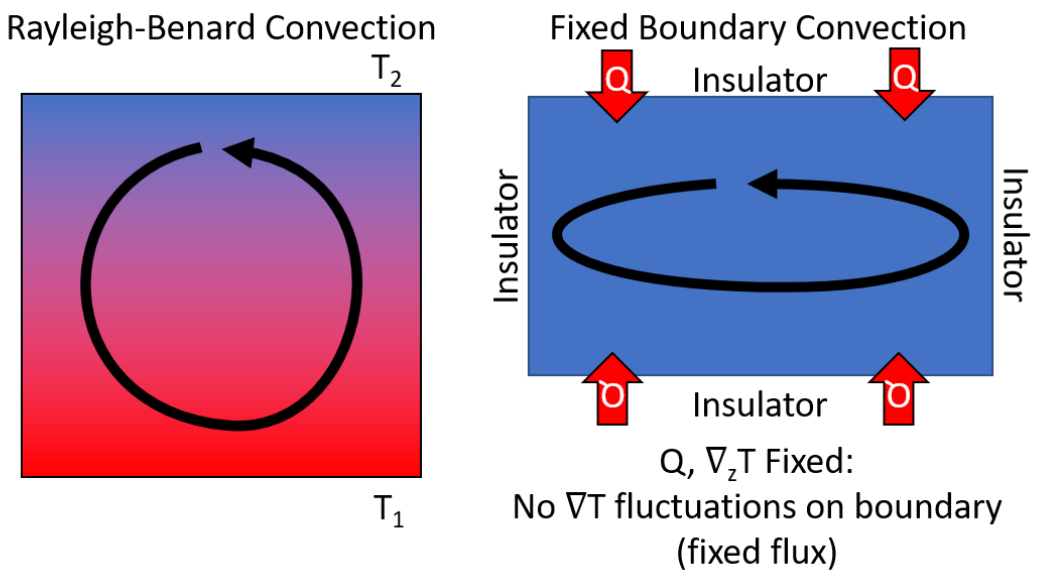

Figure 10: The fixed boundary problem (on the left) and the fixed flux problem (on the right).

important to note that the structure, parameters, and physics of the flow will be very different than the simplified case presented in the previous example. This fixed flux problem is more similar to tokamak confinement.

There are several important things to remember with respect to heating and temperature in tokamaks. First, most tokamak data, experience, and intuition is based on results which include neutral beam injection (NBI), which has dubious relevance to future devices like ITER or CFETR that will not use these beams as a primary heating source. This has introduced some initiative for "low torque" studies that aim to address this. Second, the boundary condition really matters, which is essential for calculating temperature profiles with fixed boundary conditions and other factors. Lastly, the anomalous coupling of electron-ion transfer is not studied sufficiently and remains poorly understood.

2.2 Density

The density is described with electron density n_e, ion density n_i, and impurity density n_z. These quantities are constrained by quasi-neutrality, where the sum of all charges of all species must be zero:

$$|e|n_e - z_i|e|n_i - z_z|e|n_z = 0. \tag{13}$$

The temperature will be hottest where the plasma is heated - since heating is either distributed or (usually) on-axis, the temperature profile is typically peaked in the center. In contrast, in the basic scenario, the plasma is fueled at the edge via "gas puffing", so particles go in at the edge. However,

Figure 11: Maxwell's demon [15].

unlike the temperature profile, the density profile does not peak where this gas pumping occurs - instead, the density profile peaks on the axis and decreases, as in Figure 12.

This must be a result of up-gradient transport, meaning the transport of particles is not a simple diffusion. Instead, this is the particle pinch, one of the most basic and fundamental examples of plasma self-organization, an important concept to keep in mind throughout the course. The particle flux,

$$\Gamma_n = -D_n \nabla n + V n, \tag{14}$$

has a turbulent diffusive component from the D_n term and the "pinch" contribution from the V convection component. For "interesting" behavior to occur, the signs of each of these terms will be opposite: if ∇n is negative and the diffusion is outwards, then $V < 0$. Conceptually, this is similar to the phenomena of chemotaxis observed in biophysics, where a gradient in some chemical can drive an up-gradient in flux of particles or density in a living cell. This was discovered in tokamaks by modulating gas puffing and observing the resultant density profile [14].

This convection velocity is most likely driven by the heat flux. The latter is associated with the convection velocity because the convection velocity is related to the temperature gradient; it has also been suggested that the pinch could be driven by rotation, where the torque is the source of the energy behind the pinch. However, this is limited to regimes of strong sheared toroidal rotation. Regardless of the mechanism, it is important to remember that there is no free lunch: the laws of thermodynamics cannot be violated, the spirit of Ludwig Boltzmann must be satisfied (see Figure 11), and entropy must always increase. With this in mind, most things related to the pinch are temperature gradient-driven, which is maintained by the drive heat flux, the ultimate driver behind the pinch and the up-gradient transport.

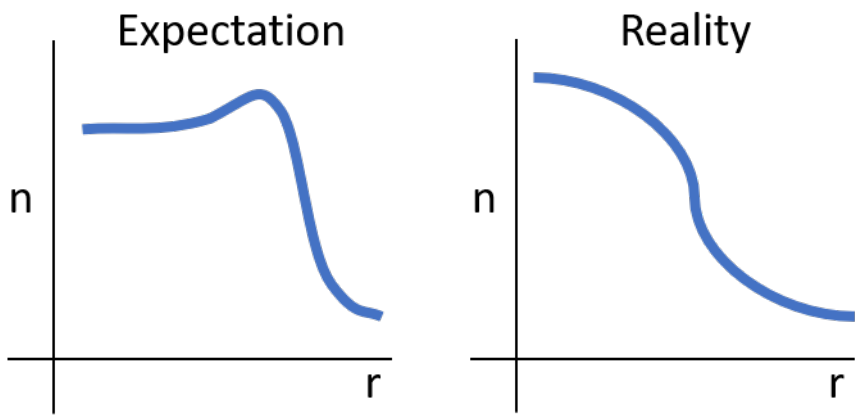

Figure 12: Intuitively, fueling at the edge might lead to a naive guess at the structure of the density profile (left) where density would be peaked closer to the source of the fueling, versus the actual structure of a density profile (right), which results from up-gradient convective transport.

Fueling and density profile formation are critical to future tokamaks - a pending question is how ITER will be fueled, with novel suggestions that range from pellet injection launched inside to plasmoids and more. Fueling remains a very active area of research.

2.2.1 Density limit

The Lawson criterion (a metric for tokamak performance which will be discussed further later on) is measured by $nT\tau_E$, the product of the density, temperature, and energy confinement time. Since density appears in the Lawson criterion, it is enticing to run towards high density to maximize performance. However, one fundamental limit on tokamak performance is the Greenwald density limit $\bar{n}_g$, which basically says you can't fuel as much as you want. The basic idea behind the Greenwald density limit is that the line-averaged (i.e. averaged through the plasma cross-section) density scales with the current, $\bar{n} \sim I_p$. This is an "engineering" constraint, with units, rather than a "physics" constraint, which should be dimensionless.

The density limit is important because approaching $\bar{n}_g$ often leads to plasma disruptions, which are not good. It is also closely related to the transport of particles, particularly at the edge plasma. This complicates the question of density and fueling, since this fundamental limit must be avoided, while still maintaining high density. Further, it also introduces a benefit to having higher current, which can, however, introduce other problems, such as disruptions.

2.3 Rotation

The plasma can rotate in the vacuum vessel. Rotation can be a consequence of external additions of momentum, or by intrinsic rotation of the plasma itself. This rotation is mostly toroidal, but the plasma can also rotate poloidally, as a consequence of symmetry.

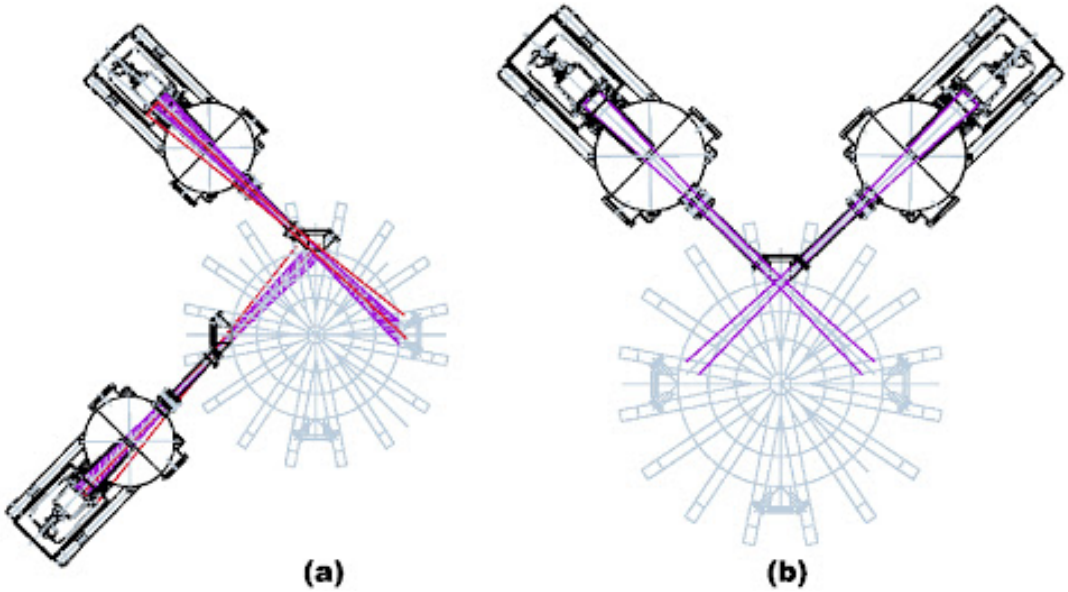

Figure 13: Sketch of neutral beam injection into the COMPASS tokamak [16].

2.3.1 Toroidal

Toroidal rotation results from either external torque (from neutral beam injection) or internal rotation (where the plasma spins itself). Neutral beam-driven rotation works by shooting a beam into the donut, as in Figure 13. The mechanism behind this process is simple and rather intuitive: shoot the beam at the plasma, the plasma spins around, in the same way as getting hit with a shotgun blast will put momentum (among other things, like density) into the target and knock it back.

Initial interest in neutral beams was focused on plasma heating, without much thought about the impact of the process on rotation. Experiments (PLT, the Princeton Large Torus) showed that neutral beams contributed to heating as intended. Later, it was realized the beams were causing rotation and influencing flow, which affected confinement from the shear in the resulting flow. This lead to an investigation of the transport of momentum,

$$\Pi = -\chi_\phi \frac{\partial \langle v_\phi \rangle}{\partial r} + ..., \tag{15}$$

where χ_ϕ is the turbulent viscosity, which was found to be similar to the ion thermal diffusivity and *loosely* similar to the density for electrostatic drift waves, $\chi_\phi \sim \chi_i \sim D_n$.

While beams provide useful heating for the plasma in smaller devices, future tokamaks like ITER cannot be penetrated by beams, which motivated plasma experiments to assess the impact of RF heating. In the late 1990s, experiments performed independently by J. Rice (Alcator) and K. Ida (JFT-2M) showed that the plasma tends to rotate spontaneously, independent of beam torque. Through spectroscopy, Rice discovered that the plasmas (heated with RF waves, rather than beams) were moving on their own. Ida used different beams with different directions and observed that the

direction of the beam mattered in overall plasma motion. This indicated the presence of some intrinsic motion, since meant that the plasma "wanted" to move on its own. This effect was observed in experiments on DIII-D and other machines, where it was shown that the torque was a result of both a dependence on an increasing pedestal pressure gradient (resulting from a residual stress created by ExB shear and driving the intrinsic rotation velocity) or increasing plasma stored energy, and at the edge in a narrow rotation layer observed near the separatrix, resulting from thermal ion orbit losses (Solomon, [17]). These experiments confirmed that if the external torque, τ_{ext}=0, the rotation $\langle v_\phi \rangle \neq 0$, meaning that the plasma exhibits "spontaneous" or "intrinsic" rotation.

This means that the total momentum flux is not simply diffusion; there is a non-diffusive stress that is driven by the pressure gradient ∇P_i, the temperature gradient ∇T_i, and the density gradient ∇n_i,

$$\Pi = -\chi_\phi \frac{\partial \langle v_\phi \rangle}{\partial r} + \Pi_{resid}, \tag{16}$$

where Π_{resid} is the non-diffusive or "residual" stress. This residual stress also depends on some breaking of symmetry (which also results for mean field magnetic dynamos). This momentum flux is not necessarily always down gradient, much like the density transport discussed in Section 2.2, and it may be related to one of the other gradients. The pressure, temperature, or density gradient could provide the energy for up-gradient momentum transport. This interdependency is an important example of tokamak self-organization.

The boundary effects are very important in this phenomenon. To spin, the plasma must conserve momentum somehow, and that momentum flows through the boundary. There is a relation between the change in the rotation and change in the energy content at the L-H transition known as "Rice scaling", where $\delta V_\phi \sim \delta w / I_p$. This allows for the pedestal intrinsic rotation.

Ultimately, the key idea here is that the heat flux produces a structure in the flow. This process is not unique to the tokamak, and is analogous to many other physical systems. In the tokamak, the heat flux makes the turbulence, which creates residual stress, which makes the flow. Likewise, in an engine, the gasoline makes a flame or burn, then the piston sets the direction, and the car moves. In the sun, there are inertially confined fusion reactions that provide the heat flux, resulting in convection in the convection zone, which generates differential rotation.

Further related to this intrinsic rotation is that there may be a flux of momentum, which results in a pinch, there is turbulent acceleration, and some intrinsic current (Lu Wang, [18]).

2.3.2 Poloidal

Poloidal rotation is neoclassical, and due to the asymmetry introduced by the curved field. It is much less significant than the toroidal rotation, and relaxes to a minimum value quickly due to the homogeneity in the field, as the interchange of flux tubes on the outside with the inside means the tube must be squeezed, requiring energy, a process described as "magnetic pumping damping". In experiment, there is some shift of the plasma from the neoclassical value detected in the absence of external torque τ_θ (meaning the beams went in toroidally), suggesting that turbulence (as the residual stress) may be contributing to something in poloidal rotation (Chrystal, DIII-D).

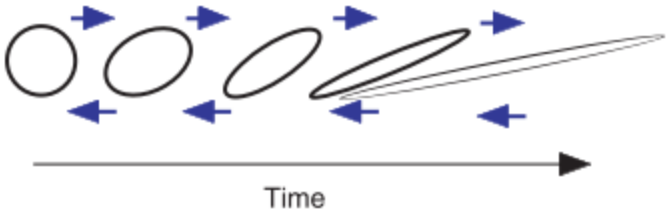

Figure 14: Shearing of the vortex. Note the shrinkage in the radial dimension. From [19].

2.4 Transport barrier

A transport barrier is a region of finite width, which must be bigger than the basic correlation length of the turbulence, $w > \Delta x_c$, (or else you couldn't see it) such that the turbulent fluxes (Q_T, Γ_T, etc.) are reduced *dramatically*. In a transport barrier, turbulence levels drop and the spectra change, but the turbulence does not go away completely. The extent to which the turbulent fluxes must drop to be considered a transport barrier is subjective, and it is important to consider (and ask, if not specified) how wide the barrier is and how much the transport changed in the barrier.

2.4.1 Self-organization

The transport barrier is critical to tokamak self-organization. The cause of the formation of a transport barrier is not fully understood, but the most likely candidate for the mechanism behind the formation of a transport barrier is some effect of a shear flow at the edge. The shear flow, v'_E, is a shear in the $v_{\mathbf{E}\times\mathbf{B}}$ velocity from the $\mathbf{E}\times\mathbf{B}$ flow. Looking at the radial ion force balance,

$$0 = \left(\frac{q}{m}\mathbf{E} + \frac{q}{mc}\mathbf{v}\times\mathbf{B} - \frac{\nabla P_i}{nm_i}\right)\cdot\hat{r}, \tag{17}$$

we can see that the balance between the electric field, Lorentz force, and pressure gradient results in enhanced shear as the pressure gradient is increased. From this equation, an increase in the pressure gradient means the electric field will become larger, which results in sharper shear from a higher $v_{\mathbf{E}\times\mathbf{B}}$ velocity, which decreases the transport and steepens ∇P further. Think of this like an eddy that is stretched, where the stretching causes it to shrink radially, reducing the step size and reducing the transport (see Figure 14).

This triggers a "feedback loop", a critical concept in self-organization in plasma; raising the heat flux leads to an increase in the pressure gradient, this raises the $\mathbf{E}\times\mathbf{B}$ velocity, which raises the shear, the shearing will cause the transport to drop, and the drop in the transport will lead the pressure gradient to increase again:

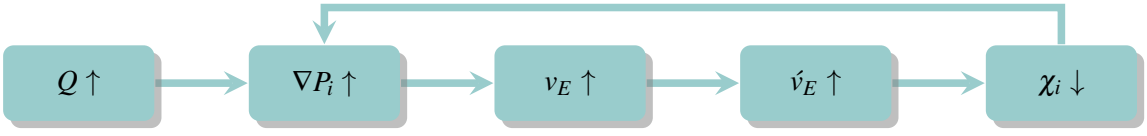

This process describes a change in a self-consistent state, and is often referred to as a transport bifurcation, which occurs at some critical pressure $P_{crit}(n, B_t, ...)$. A "bifurcation" means "two

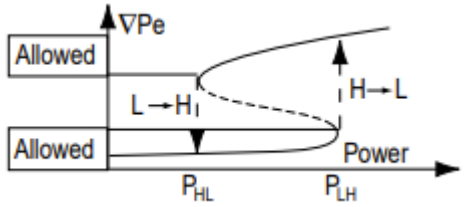

(a) A plot of power versus edge pressure gradient for the forward and back transitions demonstrating power hysteresis. The illustration shows mode hopping and critical points typical of a first-order phase transition. Note the existence of hysteresis results in regions that the plasma would pass through quickly as it jumps from one mode to the other. From [20].

(b) The letter S.

Figure 15: The S-curve.

branches" (hence "bi-fur"), meaning there are two "branches" in the behavior of a system where a drastic change in the self-organization of the system parameters occurs when some parameter reaches a critical value. Bifurcations usually manifest in plots of parameter distributions in "S-curve" shape (named because it looks like an English letter "S"), shown in Figure 15. The angled region in the middle of the "S" is usually unstable, and the top and bottom curves are usually stable. As an input parameter is varied, a bifurcation occurs when the solution spontaneously "jumps" from one stable branch to the other stable branch. This means that for the same set of input parameters, two physically sound, viable "solutions" or states of the system can exist, with the organization of that state being dependent on the state of the previous system. This is what gives the curve its characteristic "S" shape, since the two stable branches overlap, with a middle unstable region "connecting" them where no physical solutions or states exist.

2.4.2 H-Mode

In a tokamak, a transport bifurcation occurs in the transition from a low confinement regime (the L-mode) to a high confinement regime (the H-mode). This is a self-organization phenomena, where there is a spontaneous bifurcation and transition to a more organized state. The discovery of H-mode in the early 1980s is a discovery that was fundamental to the success and continuation of the fusion program [21]. The H-mode was discovered at IPP-Garching on ASDEX and presented in 1982. ASDEX (**A**xi**S**ymmetric **D**ivertor **EX**periment) was designed as a **d**ivertor experiment with good boundary control, which enabled the realization of the H-mode at modest power input, and demonstrated the importance of good boundary and divertor control, as discussed here. The H-mode revolutionized the study of magnetic confinement and motivated the study of many more improved confinement regimes.

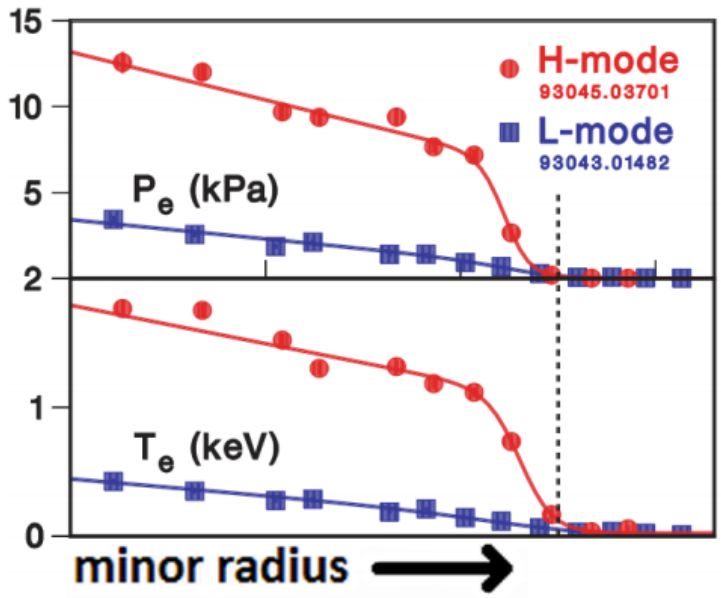

Figure 16: L-mode versus H-mode profiles for the temperature and pressure along the minor radius of the plasma (machine: DIII-D), showing the existence of an edge transport barrier near the last closed magnetic surface (indicated with the dashed line). From [22].

In very general terms, the H-mode is the spontaneous transition to a state of improved confinement with an edge transport barrier, once a critical power threshold at the edge (really, a critical heat flux of ion heat flux at the edge, acting as an edge heat pulse trigger) is reached, at $P > P_{crit}$ for power or $Q_{i,edge} > Q_{i,crit}$ for ion heat flux at the edge. This change is defined by a spontaneous transition in the profiles from "flabby" to "sharp" (see Figure 16). This leads to the formation of an extremely steep gradient layer at the edge of the plasma, which is the transport barrier; the rest of the profile "rests" above a "pedestal", which is basically the region of the steep gradient. The boundary of the pedestal is the separatrix on one side and is the maximal point of curvature in the profile on the other side. There is no agreement on what the *actual* width of the pedestal is or how it should be defined.

The ion heat flux to the edge is the "trigger" in the transition to the H-mode. Experimentally, this was shown by taking advantage of the sawtooth mode, which is a localized MHD mode within q=1. When the sawtooth "crashes", it kicks out heat that will travel outwards, essentially creating a heat pulse with a finite time of propagation to the edge. In this experiment, the power was increased slowly to just below the transition threshold, and a heat pulse was allowed to form. Once this heat pulse reached the edge, it pushed the edge heat flux over the critical value for the H-mode transition and triggered the H-mode (Wagner, ASDEX).

The transport bifurcation resulting from this transition is sketched in Figure 15 as edge pressure gradient versus input power and shown with experimental data in Figure 17 as normalized heat flux versus temperature gradient (note the change in axes - Figure 15 features a prominent "S"-shape, while the "S" is laying on its side in Figure 17). This curve indicates that there is a "turnover" point in the turbulent flux: the curved component of the "S"-curve reflects the quenched turbulence, while

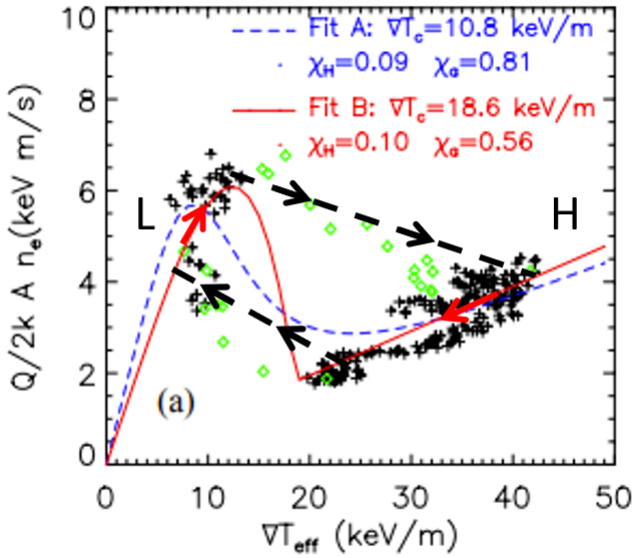

Figure 17: Normalized heat flux as a function of the temperature gradient in Alcator C-Mod. The open diamonds, traced by the thick black dashed line, indicate time points in which T_e, n_e and/or input power are changing rapidly and conditions are not in equilibrium, and are not used in fits. The curves represent best fits to the other points (+). Modified from [23].

the more straight section of the "S" corresponds to a neoclassical transport or residual turbulence. In this regime, the road "up" and the road "down" are not the same. Following the black dashed lines in each the figures, the forward transition power (or heat flux) is higher than the back transition power (or heat flux), due to hysteresis.

We will discuss the experimental data from Figure 17, but the same arguments hold for Figure 15. On this curve, there is a point where the heat flux with respect to the temperature gradient goes negative: the "rolled-over" part of the turbulent flux section, where $\partial Q/\partial(\nabla T) < 0$. This region is unstable (which is why there are no experimental data points in this area). Instead, the equilibrium experimental data lies on the stable branches, with a discontinuity in the slope between the L-mode and H-mode. This is similar to a phase change: the L-H transition can be thought of as a phase transition in the "confinement phase" of the system, rather than a thermodynamic phase change. This is reflected in experiments, where the time to the bifurcation becomes very large as the critical power is approached, a critical "slowing down" that is symptomatic of a phase transition.

The H-mode is triggered at the edge, and it is considered an "edge transport barrier", or ETB. There are internal transport barriers (ITBs) that seem to be related to the structure of the q-profile. These are of interest to ITER. This has applicability in studies of enhanced reversed shear (ERS) and negative central shear (NCS), which are related to the previous discussion of $\hat{s}$, where both shear in the electric field and magnetic field are studied. Another related variant in this discussion of flows is the zonal flow, which will be discussed further later in the course.

Figure 18: D^α signal in the DIII-D tokamak From [26].

2.4.3 ELMs

However, nothing is ever simple; where there is H-mode, there are edge localized modes (or ELMs). The term "ELM" is a bit of a misnomer, as the term "mode" typically refers to some linear instability, and an ELM is significantly more complex, nor is it affiliated with the *Ulmus* genus of deciduous and semi-deciduous trees, known as elms. Apparently, the term "ELM" was coined by Wagner (who discovered H-mode and the ELM first): in his native German, the word "elm" is related to "Elmsfeuer" or "St. Elmo's Fire" [24], which is a weather phenomena often seen at sea, where a luminous plasma is created by a coronal discharge on a rod exposed to an atmospheric electric field in a "burst", thought to resemble a tokamak ELM [25]. The Princeton term for this phenomena -"Edge Relaxation Phenomena", or ERP - provides a better physical idea of the process (and a more appropriate onomatopoeia, since "ERP" sounds like a hiccup, more akin to a violent burst at the edge than a tree), but since they didn't do it *first*, the name ELM sticks (get it?).

One of the signatures of the L-H transition is that the particle confinement becomes very good, meaning there are few particles getting out of the core plasma. This can be measured by H^α or D^α light, which are a line-width for light emission, that measures radiation produced by ionization in the divertor. This works because if there are no particles coming out, there won't be any ionization, and the light emission measurements will reflect this. In these measurements, the low-confinement mode will have a high D^α signal, and abruptly drop when transitioned to H-mode, since the particle confinement is better (see Figure 18).

As seen in Figure 18, once H-mode is reached, D^α stays down, but a burst appears towards the end of the data set; there are usually many of these "bursts" that appear in a quasi-periodic sequence in longer discharges. These bursts are ELMs: a "burst" in D^α means there is a burst of particles ejected, meaning there is something happening at the edge that kicks the particles out. There is an "ELM-free" period between the transition and the first ELM. The bursts typically do not exceed the L-mode confinement D^α readings, meaning the confinement overall stays good, despite these transient violent events.

ELMs form because of the steep gradient in the pedestal, where $\nabla P \sim \nabla P_{crit}$ or $\nabla J \sim \nabla J_{crit}$. In L-mode, steep gradients could not form because the transport was so big, but the formation of the pedestal in H-mode means there is a steep gradient, where energy is stored. From the energy principle, we can have pressure gradient-driven or current gradient-driven modes that are related to MHD instabilities: interchanges, coupling to Alfvèn waves in ballooning modes, and current-driven modes like kinks (called "peeling", since they are kinks that 'peel off' the edge of the plasma; these kinks are a consequence of the current driving a field line twist - try it for yourself

Figure 19: A plasma physics enthusiast demonstrates the kink instability.

by twisting a towel until it crimps or "kinks", as in Figure 19). Each of these processes can lead to an instability that blows off part of the edge pedestal and leads to relaxation - thus, while these ELM events are related to the proximity to the linear peeling-ballooning threshold, they are not themselves necessarily peeling-ballooning modes. There is considerable nonlinear interaction, mode coupling, and reconnection that complicate the simple association with the modes. This behavior will cycle as energy is built up and released, leading to a "sawtooth"-like, bursty behavior of an ELM cycle on the D^{α} signal.

An ELM releases a lot of energy. The steepening of the profile in the pedestal means there is a large amount of stored energy in the system, which means "knocking out" part of the pedestal (which is what the ELM is doing) releases part of that stored energy. Projections for ITER suggest that ELMs will produce roughly 20 MJ of energy in an ELM burst, which gets ejected from the plasma, into the SOL, along the field into the divertor, and directly to the PFCs. These are unacceptably high transient heat loads, and are of great concern to the engineering of the device.

3 What We Have

3.1 Lawson number

The "magic number" in tokamak physics is the Lawson number, or the fusion triple product,

$$nT\tau_E > \#_{crit}. \tag{18}$$

When considering the Lawson number, it is important to understand where these quantities in the triple product are coming from, and whether the quantities used to calculate the Lawson number were all achieved in the same plasma discharge or not. In more dubious reporting of Lawson number "records", some snake-oil scientists might take the record n, T, and τ_E of a machine and claim the product as the Lawson number, which is not a realistic metric of the capabilities of any

device. Others might use a "Lawson number equivalent", and it is important to investigate what that equivalent *is*.

We can rewrite the Lawson number in interesting ways, which illuminates the motivation behind some of the design choices in future machines. By noticing $nT = \beta B^2$, we see that the Lawson number can be rewritten as

$$nT\tau_E = \beta B^2 \tau_E, \tag{19}$$

which is why the high-field approach of Alcator or SPARC is attractive. Since β is a dimensionless physics quantity, the dimensional engineering quantity of B^2 means that higher field will give a higher Lawson number.

We can also introduce the neoclassical energy confinement time and $\tau_{E,neo}$ look at the Lawson number as

$$\beta B^2 \tau_E = \beta \tau_{E,neo} \frac{\tau_E}{\tau_{E,neo}} B^2, \tag{20}$$

which gives us two dimensionless, physics parameters (the pressure over the magnetic pressure β, a strength of DIII-D, and the ratio of the energy confinement time to the neoclassical energy confinement time $\tau_E/\tau_{E,neo} \leq 1$). Since β is dependent on pressure, which is nT, high β means high density and the β limit is related to the density limit.

This leaves engineering parameters $\tau_{E,neo}$, which is related to collisional transport and well-understood (coming from fundamental physics described by the Boltzmann equation, H-theorem, Chapman-Enskog, particle orbits, and field structure) and B^2, which is constrained by magnet technology (a historical strength of MIT, which motivated both Alcator and SPARC).

It is important to remember that the Lawson number is not necessarily the end-all-be-all in the fusion game. As emphasized by Mitsuru Kikuchi, the quest for fusion has evolved from the quest for good confinement to the multifaceted quest for good confinement, good power handling, and good boundary control. Claims of victory from reaching good Lawson number must be accompanied by some demonstration that there is a good power handling solution, which is not well defined, but provides an opportunity for the reader to invent some threshold or metric to describe power handling and become immortalized by the "Your-Name-Here" number.

3.2 Fundamental limits

By breaking down the Lawson number, we can see the fundamental physics limits in the approach to fusion. Since you can't beat the laws of thermodynamics, and the H-Theorem tells us that you can't do better than Boltzmann, our $\tau_{E,neo}$ is defined, and limits the ratio of the energy confinement time to the neoclassical energy confinement time $\tau_E/\tau_{E,neo} \leq 1$. For tokamaks, we do not worry about neoclassical transport, but for stellarators, the neoclassical transport is a concern. There is more to say about this, but it is beyond the scope of this write-up.

The β limit is expressed by β_N, or Troyon limit. The β_N limit is approximately a few (but sometimes higher) due to macroscopic instabilities (ballooning and kinks). This limit is defined by

$$\beta_N = \beta \frac{aB_T}{I_p}, \tag{21}$$

and better when below a critical value, meaning more current I_p is good, higher B_t field is bad, and bigger minor radius a is worse. The β_N limit is a good argument for compact devices, which have high current, small a, and high field.

As discussed before, the density limit appears to be an engineering limit, rather than a physics one, since it scales with $\bar{n}_g \tilde{I}_p$. However, density limits appear related to edge particle transport, and thus are intimately related to the physics of confinement. The dependence of β on density also means that this density limit influences the β limit.

These limits suggest that current I_p is good: it scales these parameters well and is good for confinement. However, the trade-off is that current also causes major problems with disruptions and difficulties in power handling.

4 Where We're Going

4.1 The present state of affairs

This brings us to the ultimate question in this business: we want good confinement, but we can't have high transient heat loads on the PFCs, so what can we do?

One (rather outdated) option is to run the plasma in L-mode, exchanging poor confinement for avoiding ELMs altogether, but that would require a huge amount of power (or current) to ignite.

There is considerable research effort devoted to mitigation or suppression of ELMs while maintaining good confinement through a technique called Resonant Magnetic Perturbations (or RMPs), invented by Todd Evans. The RMP works by putting a coil around the machine to stochasticize the edge layer of the magnetic field, which lets out some heat, but also releases particles (called "RMP pump-out"), which relieve the gradient and avoids ELMs. The catch is that the coil is difficult to engineer, and that this technique raises the power threshold for the L-H transition, meaning more power is needed to get good confinement.

Another option is the QH-mode ("Quiescent-H" mode), developed at DIII-D by Andrea Garafolo and Keith Burrell, which aims to use strong $\mathbf{E} \times \mathbf{B}$ shear at the edge to kill off all the edge instabilities. The benefit of this technique is that it creates an Edge Harmonic Oscillation (EHO), which is like a "DIY" kink at the edge of the plasma that does what the coil is doing in the RMP. The EHO is essentially a self-generated RMP, which breaks symmetry and kicks particles out, which relaxes the gradient and prevents the ELM. This process is rather delicate, making its relevance to future regimes unclear. There is also an interesting turbulent QH state.

Injection of particles to "pace" the ELMs is possible with supersonic molecular beam injection (SWIP, HL-2A) or pellet pacing (ASDEX-U and DIII-D), where small, more controlled ELMs can be provoked by injecting particles to steepen the edge pressure gradient. This technique works well, and is much more simple than RMP or QH-mode, but introduces problems with approaching the density limit, since particle injection means raising the density.

I-mode ("Improved"-mode, ASDEX-U and C-Mod) is a method which seeks to avoid ELMs, rather than mitigate or suppress them through control techniques, as with the previous methods. This can be achieved by running with the X-point in the upper divertor (rather than the lower, i.e. Figure 5(c)

flipped upside-down), which has to do with the direction of the ∇B drift. The temperature goes up at the edge, which is good for matching the boundary condition to the core, while the density stays under control, which avoids problems with the density limit. The particle confinement stays low, which is good, since the objective is to get heat, not particles, in a fusion burn. However, this regime is not fully understood, and the relevance of this regime may be questionable for reactors. While it is an interesting physics exercise, it *might* not be practical in reactor-relevant operation.

Recently, through efforts by Mitsuru Kikuchi, there has been a resurgence in interest in avoiding H-mode and focusing on getting good confinement in L-mode, without an edge transport barrier. One option for this is through negative triangularity, which offers improved confinement in the L-mode and eliminates the need for the barrier. As discussed, this works because of the favorable reorientation of trapped electron modes (a variant of drift waves), which can become basically stabilized in the negative triangularity shape (which reemphasizes the importance of shaping on both MHD and microturbulence). There may be some weak ballooning modes easily excited at the corners, preventing the transition to H-mode (Marinoni, DIII-D). Upcoming experiments at DIII-D will decide the future of this regime; as of right now, the full picture remains to be determined.

Others seem to indicate that ELMs can be mitigated entirely on ITER by simply stating that ITER will not have ELMs, though this strategy has not yet been verified as a viable method of ELM-mitigation.

Another option is to stay in H-mode and improve the divertor, and use the divertor to distribute the heat load from the bursts from the core. This is beyond the scope of this course, but underlies the importance and motivation behind the very useful and valuable field of divertor physics. Learn more at http://www.gofundme.ru/masline_PhD_thesis!

Each of these efforts points to an interesting, yet unresolved question: is turbulence good or bad? Turbulence is bad for confinement, but a little turbulence can be good, because it prevents other, larger problems.

4.2 What do we need?

At this point, we can identify the top three critical problems in the field of magnetic fusion energy: first, the self-organization of the L-H transition, with ELMs and ELM mitigation (in some capacity), second, the divertor and SOL heat flux width, and third, disruptions, which are large-scale MHD events which wipe away the current profile and lead to massive runaways, among other things, that are a result of the current.

ELM mitigation efforts focused on RMP and QH-mode will require understanding of the transport, stochastic fields, and phase evolution. The SOL and divertor heat flux problem (which will not be discussed in the course, but remains extremely important, very interesting; refer to UC San Diego MAE faculty for expertise) encompasses turbulence spreading and transport in the boundary, and is complicated by the scaling of the SOL heat flux width - that is, the width of the channel through which the exhausted power from the SOL travels and hits the divertor target. The SOL heat flux scales as $\lambda_Q \sim 1/B_\theta$ during normal (i.e. non-ELM) operation, which is not ideal; increasing the current for high β and good confinement means the heat load width shrinks, incoming heat flux is localized, and the PFC will melt. Lastly, disruptions are macroscopic MHD events that can lead to

Figure 20: The ITER device [27].

heat and current quench and runaway electrons. This is problematic because high current is good for many things but very bad for disruptions.

Other key topics, in no particular order, that must be addressed in the field, but will not be fully explored in this course:

- Impurity transport (will not be discussed)
- Energetic particles and Alfven eigenmodes: energetic particle transport and stochastisity and interaction with thermal confinement (will not be discussed; refer to UCI faculty for expertise)
- Neoclassical tearing modes (NTM): islands, transport bifurcations - related to disruptions (will be discussed some)
- RF Heating and current drive (will not be discussed)
- LH and Internal transport barriers (ITB): interest in power scaling (will be discussed)
- Particle transport and the pinch: related to fueling and the density limit. How do you fuel something like ITER? (turns out, with difficulty...this will be discussed, in depth)
- Low torque operations: How do you fuel something like ITER without neutral beams and without rotation? What about intrinsic rotation and the ripple? (will be discussed, some)

4.3 The Road Ahead

There are several major research efforts directed at magnetic confinement in toroidal devices being developed, each of which takes advantage of major guiding principles from the physics discussed in this lecture.

Figure 21: Commonwealth Fusion Systems [28].

4.3.1 Going big: High β, High β_P

The more "conventional" approach is a big tokamak with high β and high density, but modest current. This satisfies two of the factors of the Lawson criteria $nT\tau_E$, with high density n and good confinement time τ_E, and by keeping the current down, seeks to limit disruptions.

The present approach is to run at high β_p, with the poloidal field, and getting enhanced confinement with an ITB in the core and an L-mode edge. Progress has been promising, but slow-moving and incremental, raising questions about the cost of large machines. This strategy is being used in present-day tokamaks and is the motivation for even larger machines, like ITER (see Figure 20).

4.3.2 Going small: High B

The main competitor to the "going big" approach are small or compact machines with high fields, one of which is being developed as SPARC, which is a collaboration with a private company (see Figure 21) and grew out of the Alcator project. The idea is to optimize the Lawson number $\beta B^2 \tau_E$ by going for very high density (optimizing β), high toroidal field (optimizing B^2), and high current, with a reasonable confinement time τ_E.

The main advantages of this approach are that it's small, cheap, and rather simple. The main problem with this approach are disruptions, since the device needs to be run at high current to achieve this high field. Further, another critical question for SPARC is the divertor, and how it will handle the high heat loads in this small device.

4.3.3 Going twisted: The cruller approach (stellarator)

The stellarator will not be discussed in-depth, but the main idea of a stellarator is that instead of current, there is a helical magnetic field generated by helical magnetic coils. Stellarators have high

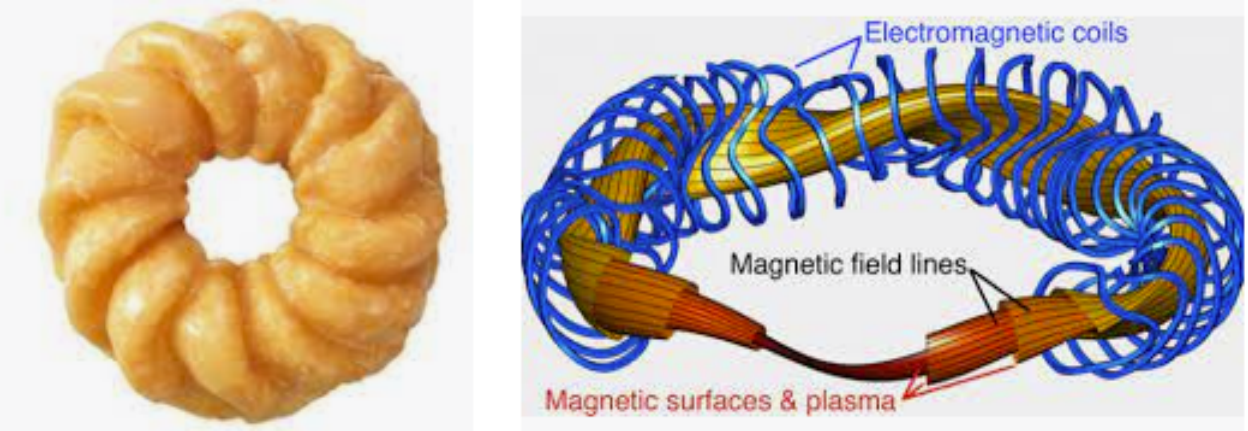

Figure 22: Two stellarators [29].

neoclassical transport, that can exceed turbulent transport, but can be reduced with optimization (German engineering). Stellarators can achieve high density so they can reach reasonable β (no current can mean a higher density limit) and good confinement time τ_E. The main problem of stellarators is the cost and complexity of building the device.

4.3.4 Going dense: Reversed Field Pinch

The RFP is a torus, but without a strong, external toroidal field. The plasma makes its own toroidal and poloidal field by Taylor relaxation. The variant on the RFP is the Quasi-Single Helicity state in the Reversed Field Pinch ("QSH-RFP", by Susanna Capello). The usual RFP is good for physics, but bad for confinement, because it is subject to MHD turbulence. The QSH-RFP gives good confinement, and has revitalized the prospects for the RFP approach.

The motivation behind the RFP is high density: similar to Greenwald, the density scales with the current, and RFP runs at very high current (much higher than a tokamak). This allows for a good Lawson number based primarily on the density alone, but improvements to the RMP through the QSH variant allow for better confinement time (and higher T). It is also much cheaper than a stellarator. The interesting question in this field is the n-scaling of the QSH state confinement.

4.3.5 Going backwards: Negative triangularity

The merits of negative triangularity configuration has been discussed in Section 1.2.1, but it deserves an honorable mention in this section as likely the most theoretically and practically promising avenue for significantly improving confinement in presently-running machines: better confinement and no transport barrier, so no ELMs. Negative T holds great promise and will be a subject of interest for the future.

References

(1) Zamperini, S.; Conlin, R. "Which tokamak is this", NFMFMHUT, 12.09.2020.
(2) Andrei Sakharov https://alchetron.com/Andrei-Sakharov, (accessed: 04.11.2021).
(3) Igor Tamm https://en.wikipedia.org/wiki/Igor_Tamm, (accessed: 04.11.2021).
(4) Chen, F. F., *An indispensable truth*; Springer: New York, 2011.
(5) Krasheninnikov, S. I.; Smolyakov, A.; Kukushkin, A., *On the Edge of Magnetic Fusion Devices*, 1st ed.; Springer: Cham, Switzerland, 2020.
(6) Krasheninnikov, S. I.; Kukushkin, A. S. Physics of ultimate detachment of a tokamak divertor plasma. *J. Plasma Physics* **2017**, *83*, 1–77.
(7) ITER Physics Expert Group on Divertor; ITER Physics Expert Group on Divertor Modelling and Database; ITER Physics Basis Editors Related content Chapter 4 : Power and particle control. *Nuclear Fusion* **1999**, *39*, 2391–2469.
(8) Kallenbach, A et al. EDGE2D modelling of edge profiles obtained in JET diagnostic optimized configuration. *Plasma Physics and Controlled Fusion* **2004**, *46*, 431–446.
(9) Vélez-Ruiz, J. F.; Sosa-Morales, M. E. Evaluation of physical properties of Dough of donuts during deep-fat frying at different temperatures. *International Journal of Food Properties* **2003**, *6*, 341–353.
(10) David, J.-L. Death of Marat, 1793.
(11) Doering, C. R. Turning up the heat in turbulent thermal convection. *Proceedings of the National Academy of Sciences* **2020**, *117*, 9671–9673.
(12) Chandrasekhar, S. Thermal Convection. *Daedalus* **1957**, *86*, 323–339.
(13) Chapman, C. J.; Proctor, M. R. E. Nonlinear Rayleigh–Bénard convection between poorly conducting boundaries. *Journal of Fluid Mechanics* **1980**, *101*, 759–782.
(14) Strachan, J. et al. A density rise experiment on PLT. *Nuclear Fusion* **1982**, *22*, 1145–1159.
(15) Physics 210B https://courses.physics.ucsd.edu/2019/Fall/physics210b/index.html, (accessed: 05.11.2021).
(16) Additional heating – Neutral Beam Injection system http://www.ipp.cas.cz/vedecka_struktura_ufp/tokamak/COMPASS/additional-heating.html, (accessed: 04.13.2021).
(17) Solomon, W. et al. Characterization of intrinsic rotation drive on DIII-D. *Nuclear Fusion* **2011**, *51*, 073010.
(18) Wang, L.; Peng, S.; Diamond, P. H. Intrinsic rotation drive by collisionless trapped electron mode turbulence. *Physics of Plasmas* **2016**, *23*, 042309.
(19) Diamond, P. H. et al. Zonal flows in plasma—a review. *Plasma Physics and Controlled Fusion* **2005**, *47*, R35–R161.
(20) Thomas, D. M. et al. The back transition and hysteresis effects in DIII-D. *Plasma Physics and Controlled Fusion* **1998**, *40*, 707–712.
(21) Wagner, F. et al. Regime of Improved Confinement and High Beta in Neutral-Beam-Heated Divertor Discharges of the ASDEX Tokamak. *Phys. Rev. Lett.* **1982**, *49*, 1408–1412.
(22) Weymiens, W. Bifurcation theory of the L-H transition in fusion plasmas, English, Ph.D. Thesis, Applied Physics, 2014.
(23) Hubbard, A. et al. *Evolution of Pedestal Profiles through the L-H and H-L Transitions in Alcator C-Mod*; 2001.
(24) Bergmann, M. German person, Personal communication.

(25) St. Elmo's fire https://en.wikipedia.org/wiki/St._Elmo%27s_fire, (accessed: 04.14.2021).
(26) Carlstrom, T. N. et al. Experimental survey of the L-H transition conditions in the DIII-D tokamak. *Plasma Physics and Controlled Fusion* **1994**, *36*, A147–A152.
(27) Giant Donut https://www.tastemade.com/videos/giant-donut, (accessed: 04.12.2021).
(28) Betty Crocker Mini Donut Maker https://www.varagesale.com/i/p27pha3m-betty-crocker-mini-donut-maker, (accessed: 04.10.2021).
(29) Stellarator Cruller https://en.wikipedia.org/wiki/Stellarator, (accessed: 04.10.2021).